LA-UR -85-3803
CONF-851009--8

LA-UR--85-3803

DE86 002435

Los Alamos National Laboratory is operated by the University of California for the United States Department of Energy under contract W-7405-ENG-36

TITLE RADIATION EFFECTS ON VIDEO IMAGERS

AUTHOR(S) G. J. Yates, J. J. Bujnosek, S. A. Jaramillo, and R. B. Walton
Teresa M. Martinez and J. Paul Black, EG&G Los Alamos and Kirtland

SUBMITTED TO 1985 IEEE Nuclear Science Symposium
San Francisco, CA
October 21-25, 1985

DISCLAIMER

Los Alamos National Laboratory
Los Alamos, New Mexico 87545

RADIATION EFFECTS ON VIDEO IMAGERS

G. J. Yates, J. J. Bujnosek, S. A. Jaramillo, and R. B. Walton
Los Alamos National Laboratory, Group P-15, MS D406

and

Teresa M. Martinez and J. P. Black
EG&G Los Alamos and EG&G Kirtland Operations
P.O. Box 809 Los Alamos, NM and P. O. Box 4339 Albuquerque, NM

Television cameras have been used successfully for telemetry of video images from remote experiments involving diagnosis of nuclear reactions. Imaging of neutrons, gamma rays and x-rays is accomplished by irradiating suitable converters that transform the incident image to a visible photon image which is then viewed by TV cameras. Frequently these cameras must operate in high radiation environments resulting from scattering of the incident beam. This exposure creates unwanted photocharge that competes with the signal produced by the visible photons, resulting in radiation-induced background buildup and spurious signals in the final image.

The primary purpose of these experiments are to (1) compare relative radiation sensitivities of several new TV imagers with Sb_2S_3 vidicons (our standard diagnostic for radiation imaging experiments) to determine if any offer greater radiation immunity with equal or better visible light sensitivity, (2) to identify reaction thresholds for given sensor types in order to specify shielding, and (3) to understand the physics involved when radiation-induced excitation occurs. The results should provide a basis for the optimum selection of TV systems for specific imaging experiments.

In the past few years several TV imagers have become available which offer improvements in speed, sensitivity, and resolution relative to conventional Sb_2S_3 photoconductor-type vidicons. The imagers tested included (1) vidicon type sensors with target materials of silicon (diode matrix), saticon (Se+Te+As), Newvicon (ZnSe), Pasecon (CdSe), Plumbicon and Leddicon (PbO), as well as Sb_2S_3, (2) silicon-based solid state arrays including charge coupled devices (CCDs), charge injection devices (CIDs), photodiodes (PDAs), (3) photoemissive image intensifiers with bi-alkali S-20 type photocathodes, including Silicon-Intensified-Target Vidicons (SITVs), proximity-focused microchannel plate tubes (MCPTs), and streak tubes. When possible, similar samples from different manufacturers were tested to determine "typical" performance for given targets. For most sensors at least two samples were measured for improved statistics.

The tests compared measurements of response to visible light and the radiation sensitivities to neutrons, gamma rays, and x-rays. All sensors showed gamma and x-ray sensitivity in the form of increased uniform background signal as shown in Fig. 1 for a silicon target vidicon. Only the silicon-based sensors showed significant neutron sensitivity. However, instead of uniform background buildup, the neutron-induced signals appear as random spurious "stars" or "speckles" in the video image, as shown for the same silicon vidicon in Fig. 2. Other imagers having approximately equal visible light imaging qualities, showed similar responses, with the CCD type being the most vulnerable and the older Sb_2S_3 vidicons the least vulnerable to either gamma rays, x-rays, or neutrons.

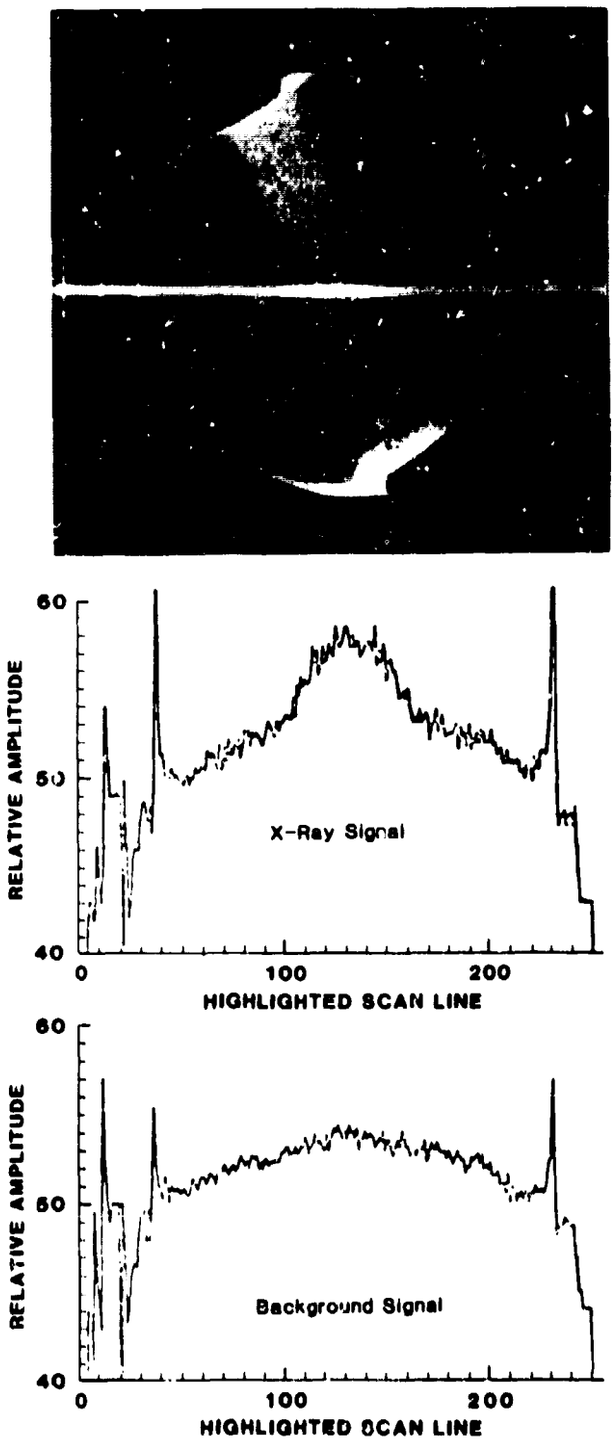

Fig. 1. Response of a vidicon with a silicon target to a 31-MR, 13-ns pulse of Bremsstrahlung photons from an electron Linac. The image shows the uniform background produced by the channel-collimated beam. Horizontal line scans through the center of images (indicated by highlighted band), taken with and without irradiation are shown in the lower portions of the figure.

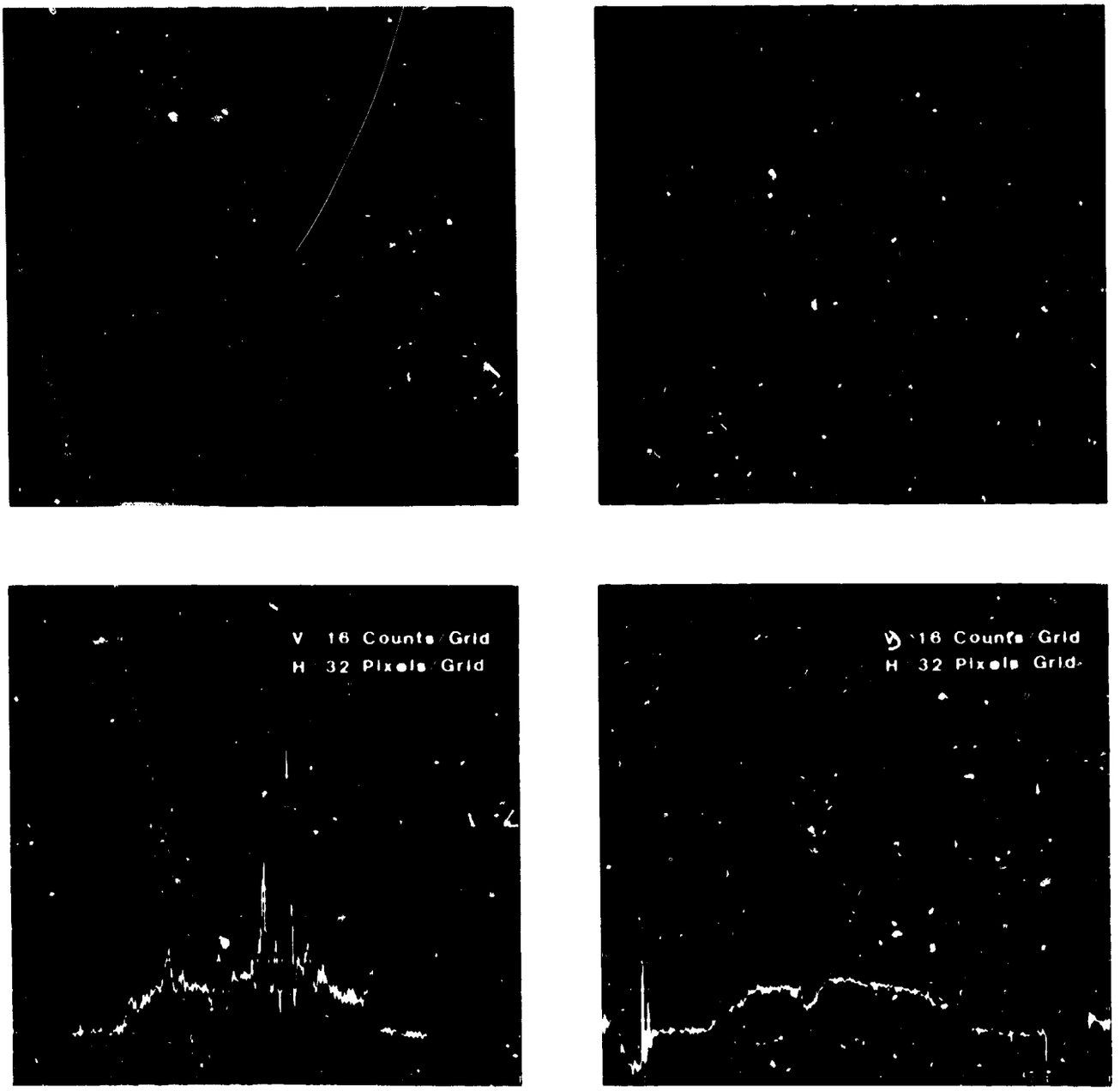

Fig. 2. Speckling effects (or "stars") produced by 14 Mev neutron interactions with a silicon-target vidicon. The images in the upper half of the figure show these effects at two different flux levels. Horizontal line scans of these images are shown in the lower portion of the figure. The grid calibrations, V and H, shown in these scan plots, refer to a 256x512 digital presentation of

RADIATION EFFECTS ON VIDEO IMAGERS

G. J. Yates, J. J. Bujnosek, S. A. Jaramillo, and R. B. Walton
Los Alamos National Laboratory, Group P-15, MS D406
P.O. Box 1663, Los Alamos, New Mexico 87545

and

Teresa M. Martinez and J. P. Black
EG&G Los Alamos and EG&G Kirtland Operations
P.O. Box 809 Los Alamos, NM and P.O. Box 4339 Albuquerque, NM

Abstract

Radiation sensitivity of several photoconductive, photoemissive, and solid state silicon-based video imagers was measured by analysing stored photocharge induced by irradiation with continuous and pulsed sources of high energy photons and neutrons. Transient effects as functions of absorbed dose, dose rate, fluences, and ionizing particle energy are presented.

Introduction

Indirect imaging of neutrons, gamma rays, and x-rays is accomplished by irradiating suitable converters that transform the incident image to a visible photon image which is then viewed by TV imagers. Scattering of the incident flux exposes the imagers to ionizing radiation. This creates unwanted photocharge that competes with the signal produced by the visible photons, resulting in radiation-induced background buildup and spurious signals in the final image.

The primary purposes of these experiments are to (1) compare relative radiation sensitivities of several TV imagers with Sb_2S_3 vidicons (our standard diagnostic for radiation imaging experiments) to determine if any offer greater radiation immunity with equal or better visible light sensitivity, (2) to identify reaction thresholds for given sensor types in order to specify shielding, and (3) to understand the physics involved when pixel excitation occurs.

Imagers Evaluated

Imagers tested included (1) vidicon type sensors with the following target materials: Sb_2S_3 photoconductors I, II, and IV, silicon diode matrix, saticon (Se+Te+As), Newvicon (ZnSe), Pasecon (CdSe), Plumbicon and Leddicon (PbO); (2) silicon-based solid state arrays including charge coupled devices (CCDs), charge injection devices (CIDs), photodiodes (PDAs); (3) S-20 photoemissive image intensifiers including Silicon-Intensified-Target Vidicons (SITVs), proximity-focused microchannel plate tubes (MCPTs), and streak tubes. Where possible, similar samples from different manufacturers were tested to determine "typical" performance for given targets. For most sensors at least two samples were measured for improved statistics.

Radiation Sources

The sources used restricted fluxes and fluences to low levels that generally produced only transient effects although some semi-permanent damage was noted for CCDs. The sources included:

(1) Continuous fluxes of 1.25 MeV (1.17 MeV and 1.33 MeV) and 662 KeV gamma rays from isotopic sources ^{60}Co and ^{137}Cs, respectively. Maximum dose rates of 77R/s were available from ^{60}Co and 0.34R/s from ^{137}Cs.

(2) 1 to 80 ns duration bursts of Bremsstrahlung photons (average energies in the 3 to 4 MeV range) produced by bombarding a 50-mil tungsten target with 8-12 MeV electrons from a Linac.

(3) Continuous flux of fission neutrons from ^{252}Cf (4×10^7n/s at the source).

(4) Microsecond duration ($\sim$ 1 to 10 μs) bursts of 14 MeV neutrons from a D-T sealed-tube generator with maximum fluence of $\approx 1.8\times10^7$n/cm^2/pulse.

(5) VanDeGraaff accelerators to produce monoenergetic neutrons in the range from 400 KeV to 10 MeV using $Li^7(p,n)$ and $H(T,n)$ reactions to study $Si(n,p)$ and $Si(n,\alpha)$ reactions in the silicon-based imagers. For neutron energies below 1.3 MeV, DC irradiations were made with maximum fluxes of $\approx 3\times10^7$n/cm^2-s. At higher energies, pulsed irradiations were made with neutron fluences of $\approx 3\times10^5$n/cm^2/pulse produced by gating the accelerator beam for $\approx$ 2 ms.

Experimental Setups and Results

Gamma Ray Measurements

Figure 1 shows the basic gamma ray irradiation setup. A one-inch diameter collimator and a 1/4-inch wide slit were used to provide contrast between irradiated and non-irradiated areas on the TV targets. Gamma ray flux levels were varied by positioning the targets at various distances from the source and by using lead bricks in the radiation path for attenuation. The video signal from the imagers was viewed on a TV monitor and recorded on an oscilloscope.

The amplifier FETS (field effect transistors) were irradiated first, without any imager in the TV camera, to determine their radiation sensitivity. No effects were observed at maximum dose rate of 77R/s.

All sensors show gamma sensitivity. Uniform buildup of background increases linearly with absorbed dose. Most sensitive are the image intensifiers which show gain behavior for gamma ray flux similar to that for visible light flux indicating the dominant gamma ray effect is to cause photoemission from the S-20 photocathode. Reverse-biasing of photocathodes or elimination of accelerating voltages virtually eliminates gamma induced signal. For non-intensified imagers, CCDs are most sensitive and Sb_2S_3 vidicons are least sensitive. A dose rate of $\approx$ 34R/s produces signal-to-noise ratios (S/N) of 93/1, 65/1, 50/1, and 1.5/1 from SITVs, MCPTs, CCDs, and Sb_2S_3 vidicons respectively. Some Sb_2S_3 vidicons are even less sensitive, producing immeasurable signal at 77R/s.

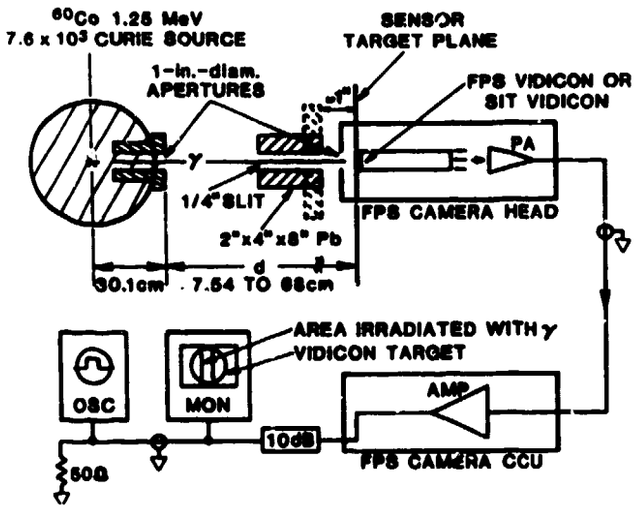

Fig. 1. The basic Cobalt 60 gamma irradiation setup. The source strength is 7.6 kilocuries.

The average S/N noted for other vidicon photoconductors was 12/1 for PbO, 6/1 for saticons, 2/1 for CdSe or ZnSe. Our measurements show that the relative visible light sensitivity at discrete wavelength bands is higher for PbO and saticon target vidicons than for those with CdSe or ZnSe. Therefore, their higher sensitivity to gamma radiation may be due to better inherent quantum efficiency. Gamma-ray sensitivity of the other silicon-based imagers, i.e., the silicon target vidicon, CID, and PDA lies between that of the above photoconductors and Sb_2S_3. The image intensifier and silicon imager responses are plotted in Fig. 2 and summarized in Table I.

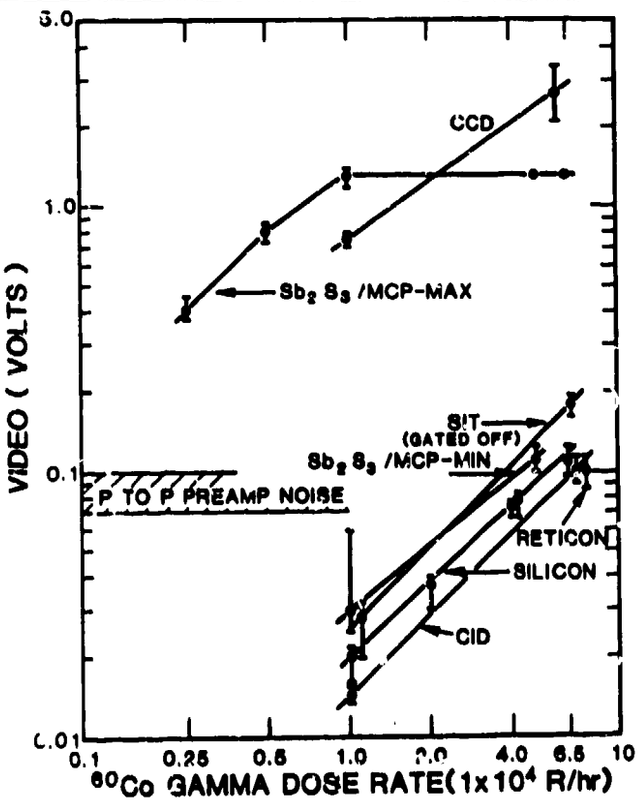

Fig. 2. Gamma ray response for silicon type TV imagers and two S-20 based image intensifiers.

TABLE I. Cobalt 60 gamma ray responses

Model #	Target	Dose Rate (R/S)	Raw data	Normalized
GE 8573A	Sb_2S_3/VID	76.5	1.5/1	1/1
RCA 8573A	"	76.5	2/1	3/1
Heimann XQ1292	"	20.2	1/1	2.5/1
EEV P8038B	"	20.2	1/1	2.5/1
EEV P849D	"	20.2	1/2	1.5/1
GE 7803 #1	Sb_2S_3/FPS	20.2	1/2	1.5/1
GE 7803 #2	"	18.6	zero	zero
Heimann AN456	Saticon/VID	20.2	2/1	5.5/1
Thomson 9950 (D)	"	20.2	2/1	5.5/1
Amperex XQ1021	PbO/VID	54.2	9/1	9/1
Amperex XQ2172 (D)	"	20.2	5/1	13.5/1
EEV P8022	"	20.2	4/1	11/1
EEV P8490 (D)	"	20.2	6/1	16/1
Heimann XQ1461	CdSe/VID	54.2	2.5/1	2.5/1
Amperex XQ1442	ZnSe/VID	54.2	2/1	2/1
GE 7803S #2	Silicon/FPS	54.2	2/1	2/1
Thomson THX 865	"	54.2	2/1	2/1
GE 17B #1	Silicon/CID	18.6	1/1	3/1
GE 17B #2	"	54.2	2.5/1	2.5/1
Fairchild 222 #1	Silicon/CCD	54.2	50/1	50/1
Reticon	Silicon/PDA	18.6	1/1	3/1
GE 7821	S-20/SITV			
(HV on)		54.2	93/1	93/1
(HV off)			<1/1	<1/1
ITT F411/GE 7803#1	S-20/MCPT-FPS			
(HV on, gated on)		54.2	65/1	65/1
(HV on, gated off)			<1/1	<1/1
(HV off)			<1/1	<1/1
CAC73435/GE7821	S-20/STK-SITV			
(STK HV on, gated on, SIT HV on)		54.2	240/1	240/1
STK HV off, SIT HV on)		15.0	25/1	2/1
(STK HV on, gated off, SIT HV on)		54.2	2/1	90/1

Bremsstrahlung Irradiations

Similar collimation and slit arrangement was used to provide contrast in the video signal. The Linac was synchronized to the TV sync and pulsed once every fifth TV field, giving essentially single pulse response. The dose per pulse was measured by exposing thermoluminescent dosimeters (TLDs) at the TV target plane. The response for a silicon target vidicon to ≈ 31 millirads exposure from a 13 ns FWHM x-ray burst is shown in Fig. 3. The S/N (≈ 5/1) observed for this dose is in good agreement with S/N (≈ 6/1) from ≈ 36 millirads time-integrated 3 ms (TV fld period) dose from ^{60}Co gammas, indicating a dependency on total dose rather than on dose rate. The x-ray response for this sensor is linear between 31 and 865 millirads with saturation occurring at ≈ 1.1 rads. A 26 ns FWHM, 62 millirad exposure caused saturation in the CCD imager, indicating ≈ 18x higher x-ray sensitivity for this sensor.

Neutron Irradiations

For the unintensified imagers, only the silicon-based units show significant neutron sensitivity. Neutrons produce spatially random excitation of individual pixels (see Fig. 4) with little or no background buildup. The S-20 MCPT/Sb_2S_3 intensifier showed no individual interactions, but showed background buildup (Fig. 5) similar (S/N ≈ 10/1 from 1.8×10^7 n/cm^2) to its gamma response (S/N ≈ 45/1 from 1×10^8 /cm^2).

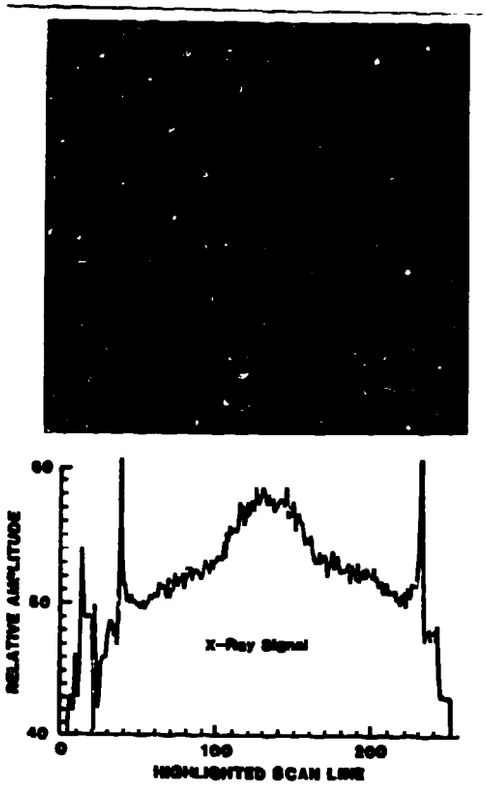

Fig. 3. High energy photon induced signal in silicon-target FPS vidicon.

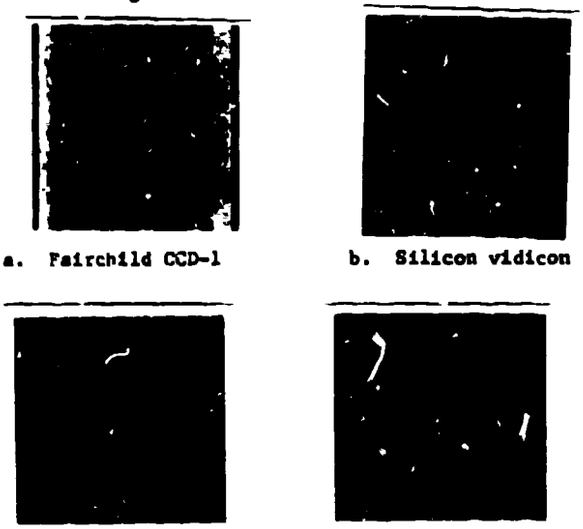

a. Fairchild CCD-1

b. Silicon vidicon

c. GE CID

d. Reticon

Fig. 4. Neutron-induced speckling for several silicon-based TV imagers when irradiated with 14 MeV fluence of $\gtrsim 4.5 \times 10^5 n/cm^2$.

The expected number of individual interactions from silicon neutron cross-section calculations agrees well (within experimental accuracy and limited statistics available) with observed counts (see Table II for 14 MeV response) of affected pixels for all silicon imagers. Again, CCDs are the most sensitive imagers ($\geq$ 1135 interactions from $4.5 \times 10^6 n/cm^2$). Pulse height and area distribution of excited pixels for CCD #1 from pulsed irradiation with monoenergetic neutrons of 4, 6, 8, and 10 MeV are found in Table III and Fig. 6. Comparing the 6 and 8 MeV data with the 4 MeV data shows the relative contributions of (n,p) and (n,α) reactions. Excitation with ^{252}Cf fission spectrum neutrons produced a smaller ratio of saturated pixels versus total affected pixels than ratios obtained from higher energy neutrons.

Reduction of radiation effects by shielding was investigated. Star effects in the silicon vidicon, amounting to 33 stars from an exposure of $2.8 \times 10^5 n/cm^2$, were essentially eliminated by shielding with either 30.5 cm of polyethylene or 9.2 cm of tungsten. These shields represented 2-3 mean free paths for the attenuation of 14 MeV neutrons.

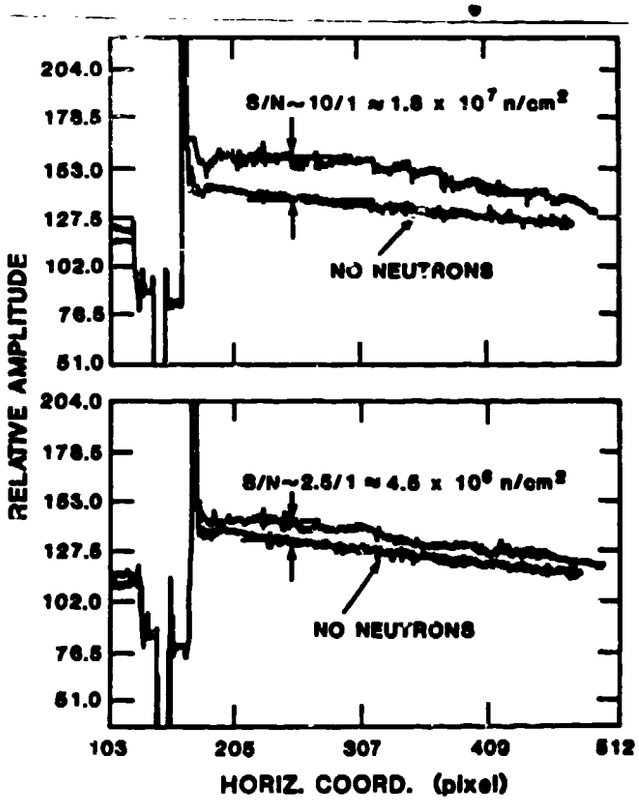

Fig. 5. Neutron-induced background (with no speckling) in S-20 based image intensifier from irradiation with 1-10 μs bursts of 14 MeV neutrons.

TABLE II. Events induced in silicon imagers from 4.5×10^6 14 MeV neutrons/cm^2

Model #	Total # of Pixels	Pixels/cm^2	Total Events
GE 7803S/FPS	1.8×10^6	1.4×10^5	336
FE-222/CCD	185,480	1×10^5	1135
GE17B #1	96,228	1.57×10^5	108
Reticon/PDA	1×10^4	0.5×10^5[18]	18

The effective number of pixels/cm^2 for CCD #1 reflect approximately 50% insensitive area between pixels. For the silicon vidicon, effective pixel area is the $\gtrsim$ 30 μm-diameter electron beam, rather than the 7 μm diameter silicon diode.

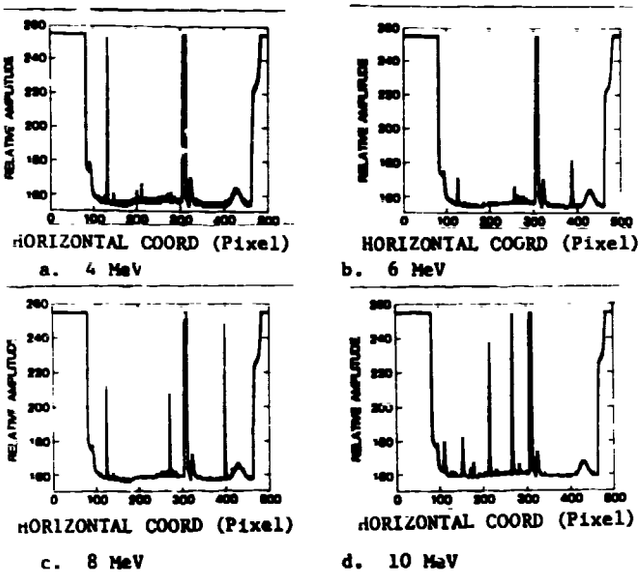

Fig. 6. CCD video lines through affected pixels. Each plot is an overlay of three random lines.

Table III. Pixel area and amplitude distributions from neutron induced speckling in CCD #1 from $3x10^5$ n/cm^2 fluence.

	4 MeV	6 MeV	8 MeV	10 MeV
Pixels	52	42	85	$1.2x10^3$
Area range	1-4	1-6	1-6	1-22
Avg. area	1.6	2.6	4.0	6.2
Ampl range	165-210	166-227	165-256	165-256
Avg. ampl	170	191	175	175

Correlation Between Measurements and Calculations

Several reactions of neutrons with silicon nuclei that produce ionizing particles include elastic and inelastic scattering, (n,p) and (n,). The particles create electron-hole paris as they pass through the silicon substrate. Carriers produced in device depletion regions, or within a diffusion length of these regions, are stored as photocharge which is readout later as video signal from the TV imager. Because of the short range of scattering recoils and charged secondary particles, most of the energy deposited as ionization occurs within the material where the reaction occurs. Consequently a single reaction can show up as a local effect or a star in one or a few contiguous pixels on the TV imagers. In contrast, the energy loss per unit distance of electrons produced by the interaction of high energy gamma rays is smaller, resulting in the more uniform general background build-up noted for photon irradiations.

The range of video signal amplitudes measured from the noise level to saturation (where the charge) may be stored by several neighboring (pixels) are consistent with calculations of the number of electron-hole pairs produced as a function of incident neutron energy and the pixel sensitivity, (a function of amplifier noise and target quantum efficiency), and the charge capacity (the number of electrons/well for solid state imagers or holes/diode for silicon-target vidicons). The noise threshold range for the various imager/amplifier combinations corresponds to 25 to 100 electrons and estimates of pixel charge capacity (1,2,3) range from > 10^3 to > 10^6 electrons/pixel. One study (4) reports that 1) recoils in the active silicon region produced by neutron scattering produce from $\sim 7x10^{-20}$ to $3.2x10^{-19}$ C/mm^3 per n/cm^2 for neutron energies from $\sim$ 300 KeV to 4 MeV, increasing to $\sim 6x10^{-19}$ C/mm^3 per n/cm^2 at higher energies, and 2) (n,α) and (n,p) reactions produce from about $1x3x10^{-20}$ C/mm^3 per n/cm^2 at $\sim$ 4 MeV increasing to $\sim 2x10^{-18}$ C/mm^3 per n/cm^2 in the range from 8 MeV to 14 MeV. The resulting total range is $\sim 7x10^{-20}$ to $5.4x10^{-18}$ C/mm^3 per n/cm^2. The effective Si volume/pixel is $\sim 3x10^{-6}$ for silicon vidicons and $\sim 2x10^{-5}$ mm^3 for CCD and CIDs used in this study. Using the $3x10^5$ n/cm^2 fluence from the VandeGraaff experiments and the above range of possible charge, gives $\sim$ 2.6 to 508 e-h pairs/pixel for CCDs or CIDs and $\sim$ 0.4 to 77 e-h pairs/pixel for silicon vidicons. We believe this to be expected average charge/pixel, but because only a small fraction of the total pixels are affected, their actual charge/pixel is much larger. Examination of the CCD data from Table III shows $\sim 1.2x10^3$ affected pixels out of $1x10^5$ available pixels giving 83x average charge or 217 to $4.2x10^4$ e-h pairs pixel, which is sufficient to produce signals from noise to saturation for this imager.

Acknowledgements

The authors wish to acknowledge help with gamma ray measurements provided by R. Head of EG&G Las Vegas; help with neutron measurements provided by L. Sprouse, P. Weiss of Los Alamos National Laboratory and B. Simmons of Sandia National Laboratory; help in neutron reaction calculations and measurements provided by B. Noel, R. Haight of Los Alamos National Laboratory and J. Kammarraad of Lawrence Livermore Laboratory; help with data reduction by R. Liljestrand, M. Lopez, and M. Chavarria of EG&G Los Alamos.

References

1 G. J. Yates, High Resolution SIT TV Tube for Subnanosecond Image Shuttering, Los Alamos National Laboratory report number LA-9771-MS, September 1984, pp. 10-15 and pp 73-75.

2 J. M. Killiany, Radiation effects on Silicon Charge-coupled Devices, IEEE Transaction on Components, Hybrids, and Manufacturing Technology, Vol. CHMI-1, No. 4, December 1978, pp. 275-287.

3 A. Bross, High Resolution, Position sensitive Solid State Detectors Utilising the CCD Concept, Silicon Detectors for High Energy Physics, proceedings of Fermilab workshop, Oct. 15-16, 1981, pp. 127-148.

4 R. Kuckuck, Semiconductor Detectors for Use in the Current Mode, Lawrence Radiation Laboratory Report #UCRL-51011, February 10, 1974, pp. 10-13.